

95  
96

## SIMULATION OF BRITTLE FRACTURE via MOLECULAR DYNAMICS

WILLIAM G. HOOVER

### 1. SYNOPSIS

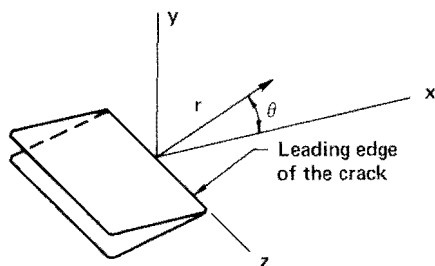
Fast fracture in brittle materials can be simulated with molecular dynamics. The results have many features in common with macroscopic experiments on real materials. These features include steady propagation of cracks at speeds comparable to the speed of sound; increasing crack velocity with increasing stress; crack "inertia", allowing the penetration of cracks into regions which would not fracture under static conditions; and crack-surface irregularity at moderate-to-high temperatures.

### 2. INTRODUCTION

The breaking of an object into two or more pieces is fracture. The economic consequences of fracture in jet aircraft, bridges, and oil shale, for instance, abundantly justify the study of fracture from a variety of viewpoints. These studies range from microscopic trajectory analysis of atoms near crack tips, through mesoscopic analyses of the formation and motion of dislocations and voids, to macroscopic finite-element or finite-difference simulations of failure for materials characterized by "damage functions" or other failure criteria describing susceptibility to fracture.

Fracture normally occurs through the enlargement of existing defects in solids--voids, grain boundaries, micro-cracks, or surface irregularities.

All such defects concentrate stress. The fact that failure stresses lie far below ideal crystal strengths shows that the stress concentration is large. It is not hard to see, from continuum elasticity theory, that a sharp crack has an infinite stress concentration. The crack shown in Figure 1 has a



DISPLACEMENTS:

$$u_x = \cos(\theta/2)f(r)g(\theta) ;$$

$$u_y = \sin(\theta/2)f(r)g(\theta) ;$$

$$f(r) = (K/2G)(r/2\pi)^{1/2};$$

$$g(\theta) = 1 + 2\sin^2(\theta/2) ,$$

for  $\lambda = \eta$ .

Figure 1. Crack in an elastic continuum<sup>1</sup>

displacement  $u_y$  in the vertical direction of order  $(K/G)x^{1/2}$ , where K is the "stress-intensity factor," G is the shear modulus, and x is the horizontal distance from the crack tip. The strain and stress both diverge as  $r^{-1/2}$  at the crack tip. This singular behavior is unpleasant because many discrete zones are needed near the crack tip to give an accurate numerical description of the displacements and strains. Because interatomic forces are finite, it can be anticipated that the singularity changes form very near the crack tip. Atomistic simulations of fracture show how this comes about.

The classical Griffith model of fracture is based on energy conservation. Consider the application of the model to a strip undergoing fracture. The unbroken part of the elastic strip shown in Figure 2 has been stretched by an amount  $2ch$  vertically, so that its energy density  $e$  is  $(2\eta+\lambda)e^2/2$ , where  $\eta$  and  $\lambda$  are the Lamé constants.

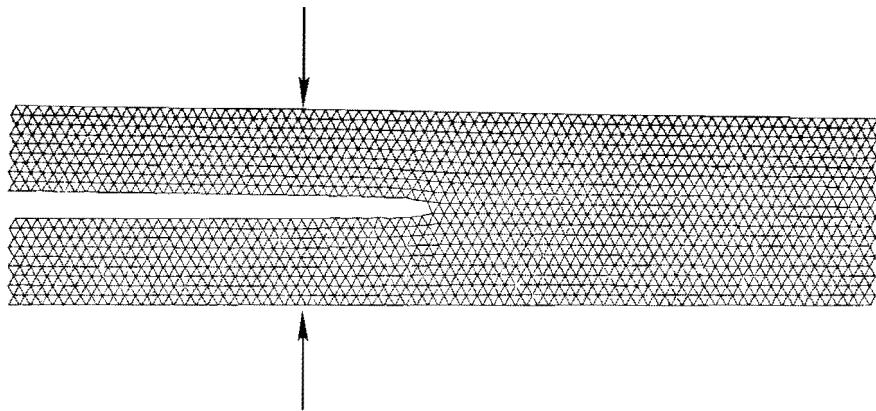


Figure 2. Elastic strip undergoing brittle fracture. Strip width is  $2h$ .

The broken portion is stress free but has a surface energy, per unit length of surface  $\gamma$ , equivalent to an energy density  $\gamma/h$ . Griffith suggested that simple energy minimization causes fracture to propagate when the strain energy matches the surface energy:

$$\sigma_G = (2\eta + \lambda)^{1/2} (2\gamma/h)^{1/2} = (2\eta + \lambda)\epsilon_G \quad . \quad (1)$$

This Griffith model is only an approximation. It ignores the irreversible nature of fracture, the sensitivity of fracture to temperature, and the dependence of crack-surface morphology on both temperature and velocity. Griffith's model always underestimates the failure strain, but it is still a useful semiquantitative guide, as we will see.

### 3. ATOMISTIC MODELS OF FRACTURE

A microscopic atomistic model for crack structure or growth requires (1) a force-law, (2) equations of motion, and (3) appropriate boundary conditions. For simple closed-shell atoms--argon is the prototype--the forces are well understood. For metals the situation is complicated, even for bulk matter. When empirical potential functions are fitted to bulk properties it is not unusual to find that defect properties are in error by as much as a factor of two.<sup>2</sup> Despite intense theoretical effort it appears highly unlikely that fundamental quantum-mechanical estimates of metal forces will prove useful soon. Instead, there is considerable room for judicious empirical work. An approach fitting all possible data (elastic constants, formation, fusion, surface, vacancy and stacking-fault energies, etc.) with short-ranged forces might work. At present it is unreasonable to expect quantitative agreement between computer simulations and experiment--the forces are simply not well enough known.

It is still possible to develop techniques for simulating brittle fracture by studying model systems with simple forces. This is the point of view we have adopted in studying fracture.<sup>3,4</sup> It is a particularly fruitful approach to follow in characterizing number-dependence, sensitivity to boundary conditions, and the qualitative response of brittle cracks to stress gradients and other lattice defects. Because plastic deformation involves the long-range interaction of many dislocations, plastic "ductile" fracture is best handled from either the mesoscopic or macroscopic point of view.

The simplest force law useful in treating fracture problems is the piecewise-linear ("Hooke's Law") force illustrated in Figure 3.

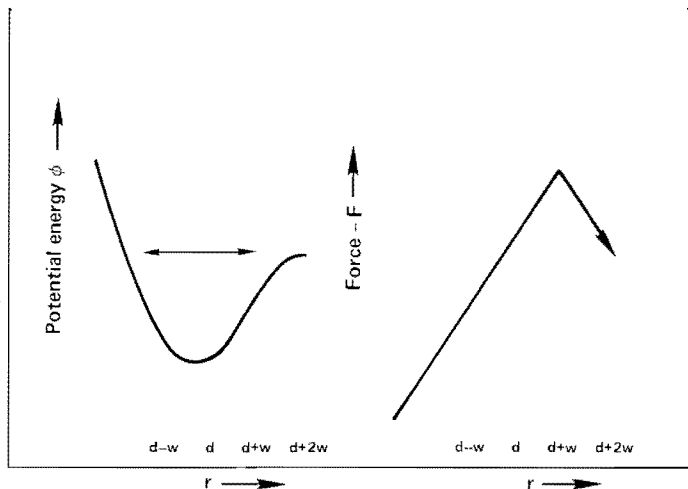


Figure 3. Potential and force used in fracture simulations.

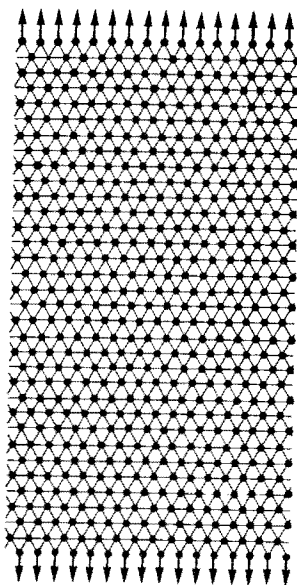


Figure 4. Fixed-stress boundary.

The atom-atom potential has its minimum at  $r=d$ . The force resisting separation increases with  $r$  up to the mechanical instability point at  $r=d+w$ . The force then falls linearly for larger  $r$ , and vanishes for  $r \geq d+2w$ .

Fracture calculations for this potential have been carried out using both fixed-stress<sup>3</sup> and fixed-displacement<sup>4</sup> boundary conditions. In the fixed-stress case 512-atom crystals, periodic in the  $x$  direction, were stressed in the  $y$  direction as shown in Figure 4.

The potential energy  $\Delta\Phi$  taken up by such crystals<sup>3</sup> with a crack of length  $L$  is shown in Figure 5. The interparticle force constant is  $k$ , and the interparticle spacing is  $d$ . The energy data extrapolate smoothly to the elastic-

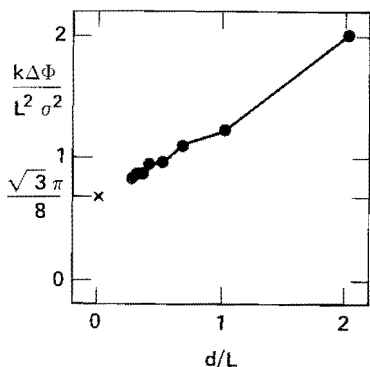


Figure 5. Energy Increase in a 512-particle stressed crystal.

theory result (marked with an x).

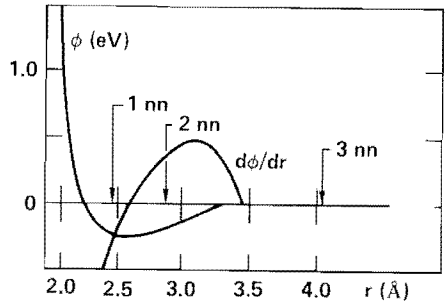
Fixed-displacement boundaries have been studied for the same force law. The crack shown in Figure 2 has all atoms on the top and bottom boundaries fixed, in order to produce a macroscopic vertical strain  $\epsilon_{yy}$ . In this case too the energy extrapolates smoothly to the elastic-theory prediction as the number of atoms is increased. For the two kinds

of boundary conditions shown in figures 2 and 4 the stress at which a long crack will propagate can be calculated. By considering crystals of from 700 to 10,000 atoms the limiting value of this failure stress, and thus the critical stress-intensity factor  $K_C$  was calculated with an accuracy of 1 part per thousand.<sup>4</sup> The results obtained by the two methods agreed nicely. The cracks require a stress exceeding the Griffith stress  $\sigma_G$  by about 26%. The excess energy, beyond the surface energy, ends up as thermal motion, or "heat", the signature of an irreversible process. A part of the excess energy can be used to drive fracture at stresses below the static value. The specimen shown in Figure 2 actually has a slight taper. The slope of the upper boundary is -0.016. The arrested crack passed beyond the point of

arrest predicted from static analysis (indicated by arrows). A series of such calculations resulted in final arrest at stresses ranging from 2 to 12% in excess of the Griffith stress. This commonly observed feature of real cracks can occur only when the Griffith stress lies below the static failure stress.

#### 4. ATOMISTIC MODELS FOR FRACTURE IN IRON

Most three-dimensional fracture models have dealt with the cleavage fracture of body-centered cubic Iron.<sup>2,5,6</sup> The body-centered lattice is unstable with nearest-neighbor forces (it is a worthwhile exercise to find the shear direction demonstrating this). Therefore a potential linking second neighbors is required. The



Johnson potential is most commonly used. It is shown in Figure 6.

This potential underestimates the surface energy by about a factor of two, but is otherwise useful in suggesting the additional complexities associated with three-dimensional simulations. To avoid using more than a few hundred particles, only the crack tip is described, by fixing either the displacements or the forces on the boundary particles. More sophisticated models couple the boundaries to an elastic continuum which can incorporate realistic boundary conditions. In most cases the crystals studied have been only one unit cell in thickness, and, typically, there is no mechanism for the relief of stress in the thickness direction or for the formation of jogs which might reduce the stress required for fracture.

Mullins<sup>6</sup> has studied the dynamics of crack tips propagating at stresses ranging from 20 to 70% above the Griffith stress. Evidently the minimum stress required for fracture, using the Johnson potential, is close to that found in two dimensions, namely between 1.2 and 1.3 times the Griffith stress. Mullins found propagation speeds ranging from 20 to 55% of the transverse sound velocity, as shown in Figure 7. These speeds lie somewhat below those

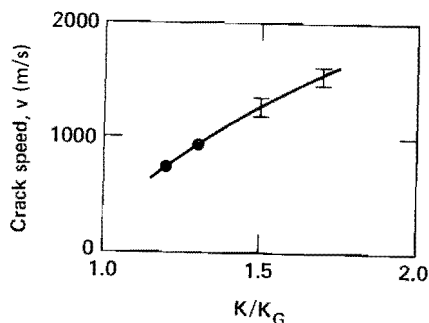


Figure 7. Crack velocity for iron.

found for the two-dimensional Hooke's-Law forces, and agree well with fracture data on steel.

There appear to be no computational difficulties in extending Mullins' work to include defects in the vicinity of the crack tip. The main problem lies in the uncertain nature of forces in real metals.

## 5. DYNAMIC STRESS INTENSITY FROM SHADOW PATTERNS

During the past ten years Kalthoff's group at Freiburg has studied dynamic fracture, in metals and plastics, using "shadow patterns". The propagation of a crack down the length of a specimen produces a moving cusp-like dimple around the crack tip. When transverse light is reflected from the specimen (as with steel) the moving dimple results in a bright "caustic" ring which can be photographed. For elastic materials, the size of the ring can be related directly to the stress intensity factor--i.e., the stress  $\times (2\pi r)^{1/2}$  directly in front of the crack tip. If the light is transmitted (as with transparent plastics), the dimpling acts as a lens and a similar moving ring appears behind the specimen.

By tracking the size and motion of the caustic ring Kalthoff's group has obtained considerable data indicating wide variations in stress about that which could be calculated on a static basis. Because the data indicate that fracture sometimes propagates at stresses lower than the critical static value, a quantitative understanding of the shadow pattern results has been sought by the Electric Power Research Institute.<sup>4</sup>

To what extent can shadow patterns be duplicated from atomistic simulations? This question has been studied by Moran.<sup>4</sup> By using the plane stress elastic equations to calculate displacements normal to his two-dimensional crystals, Moran could represent the surface of a three-dimensional thin fracturing strip. Next, by simulating the reflection of light from the triangular mirrors aligned according to the elastic equations, he simulated the light pattern which would be photographed in a shadow-pattern experiment. Figure 8 is a series of shadow patterns formed as the first seven bonds break. Individual sound waves can be seen spreading out from the moving crack tip.

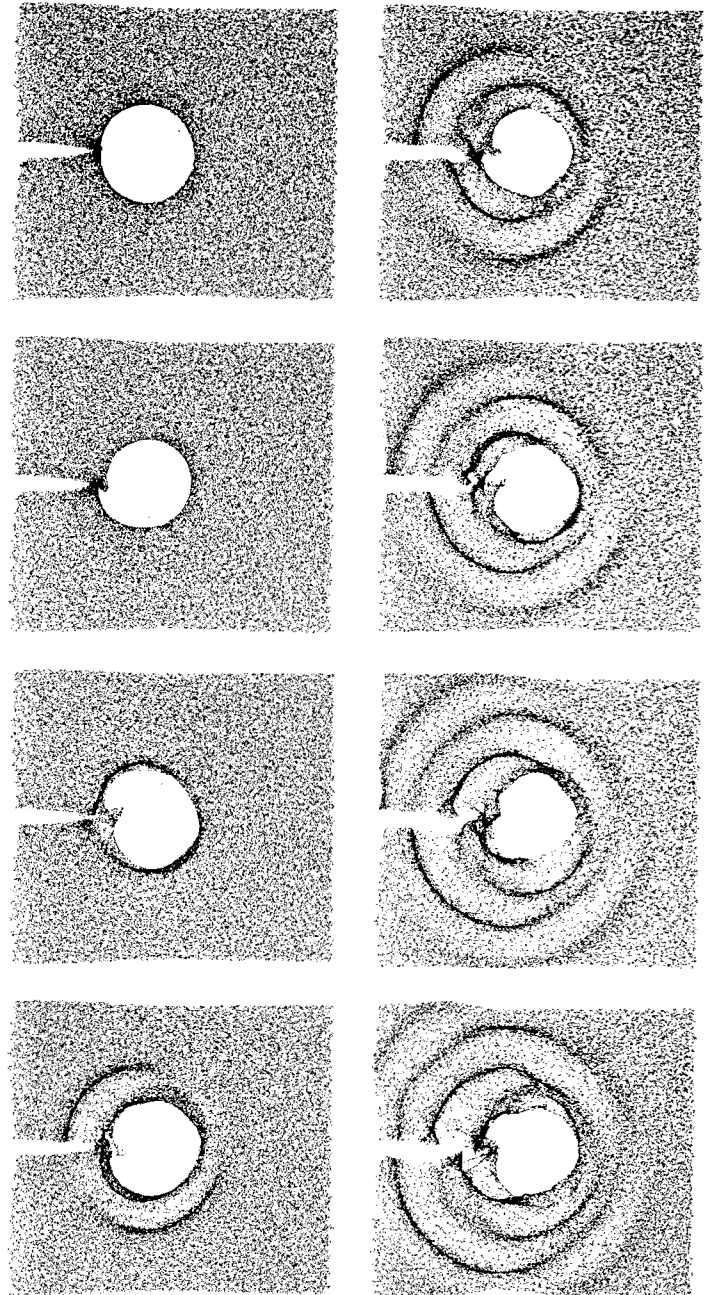


Figure 8. Shadow patterns for cracks with  $(\Delta L/d) = 0, 1, 2, 3, 4, 5, 6, 7$

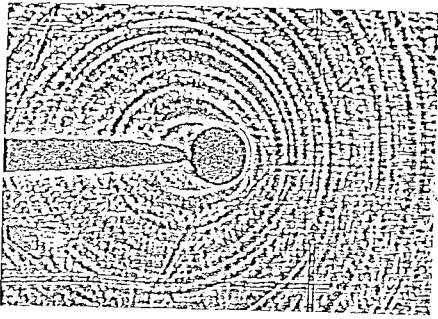


Figure 9. Experimental shadow pattern for steel.

Figure 9, taken from Kalthoff's work, is a reproduction of an experimental shadow pattern in high strength steel.

The quantitative analysis of the shadow patterns is somewhat disappointing. The static caustic agrees well in size with the expected value from elastic theory. The irregularity in the dynamic results

(and those shown in Figure 8 were obtained with a slight viscous damping added to the equations of motion) makes quantitative comparison with experiment impossible. The steady-state caustic diameter is essentially indistinguishable (within nearly 10% fluctuations) from an estimate based on static theory.

## 6. DUCTILE FRACTURE

Except at low temperature, real metals normally fracture by a ductile mechanism. Voids form and coalesce as shear stress generates and moves lattice dislocations. When "plastic flow" has occurred the failed parts no longer fit together after fracture. Because real metals are made of atoms, there is no doubt that a sufficiently large atomistic model could describe ductile failure too. But how large? In ductile failure material millimeters away from the crack surface undergoes extensive plastic flow. A cubic millimeter of iron contains about  $10^{19}$  atoms. Even a square millimeter exceeds current computational capacity by six orders of magnitude.

Thus the study of models following the detailed atomistic motion of dislocations is not feasible, and a continuum macroscopic approach is used instead. Rather than solving Newton's ordinary differential equations of motion,

$$m\ddot{a} = F \quad , \quad (2)$$

we solve instead the partial differential macroscopic equation of motion,

$$\rho \ddot{a} = \nabla \cdot \sigma \quad , \quad (3)$$

where  $\sigma$  is the stress tensor. The finite-difference method involves approximating the continuum by a discrete set of nodes (or contiguous zones) and moving these according to ordinary differential equations. If, for instance, a two-dimensional elastic continuum is divided into triangular zones (See Figure 2), and the displacement in each zone varies linearly with position, the continuum equation (3) reduces to equations (2) where the force is given by Hooke's Law.<sup>3</sup>

To treat fracture by continuum methods, a criterion for the breaking of nodal links or the separation of contiguous zones must be specified. Wilkins<sup>7</sup> has successfully used a "damage function" depending upon plastic strain and pressure as a failure criterion. Popelar and Gehlen equated the (potential) energy lost in discarding a stressed crack-tip zone to the new surface energy gained. The surface energy was a specified function of crack velocity. Other empirical approaches have been based on crack-tip radius or crack-opening displacement. Such empirical approaches can successfully correlate data for particular classes of experiments, but are not sufficiently sound to make

trustworthy predictions for new geometries. A major computational difficulty is the necessity to specify in advance possible crack trajectories.

The fundamental mechanism for the propagation of ductile fracture is the growth and coalescence of voids ahead of the crack tip. The detailed numerical simulation of fracture incorporating these voids has not yet been seriously attempted.

## 7. OUTLOOK

Empirical short-ranged potential functions, chosen to reproduce bulk and defect properties, coupled with Mullins' boundary conditions, should help in understanding crack-tip phenomena--stress corrosion cracking, dislocation production, and the interaction of cracks with voids. The prospects for fundamental progress on ductile fracture are more remote. As a start, more emphasis on mesoscopic simulations is recommended.

## 8. PROBLEMS

1. Show that the shear modulus in a face-centered cubic lattice with nearest-neighbor Hooke's Law forces is not isotropic.
2. Show that the Griffith far-field stress for a triangular-lattice strip, of width  $2h$ , with nearest-neighbor interaction energy  $-e$  is  $(3\sqrt{3}\kappa e/2h)^{1/2}$ , where  $\kappa$  is the nearest-neighbor Hooke's-Law force constant. Hint: show first that the lattice is elastically isotropic, with both Lamé constants  $\eta$  and  $\lambda$  equal to  $\sqrt{3}\kappa/4$ .

## REFERENCES

1. J. R. Rice, "Mathematical Analysis In the Mechanics of Fracture," In Fracture, II, Chap. 3 (Academic, 1968).
2. B. deCellis, A. S. Argon, and S. Yip, J. Appl. Phys. 54, 4864 (1983).
3. W. T. Ashurst and W. G. Hoover, Phys. Rev. B 14, 1465 (1976).
4. B. Moran, Crack Initiation and Propagation In the Two-Dimensional Triangular Lattice, Ph.D. Dissertation (Univ. of Ca. at Davis, 1983)
5. P. C. Gehlen, G. T. Hahn, and M. F. Kanninen, Scripta Met. 6, 1087 (1972).
6. M. Mullins, Scripta Met. 16, 663 (1982).
7. M. L. Wilkins, "Fracture Studies with Two- and Three-Dimensional Computer Simulation Programs", Lawrence Livermore National Laboratory Report UCRL-78376 (1977).
8. C. H. Popelar, and P. C. Gehlen, Int. J. of Fracture 15, 159 (1979).